

Charmonium potentials: Matching perturbative and lattice QCD

Alexander Laschka, Norbert Kaiser, and Wolfram Weise

Physik Department, Technische Universität München, D-85747 Garching, Germany

(Dated: August 15, 2012)

Central and spin-spin potentials for charmonium, constructed from Nambu-Bethe-Salpeter amplitudes in lattice simulations of full QCD, are matched with results from perturbative QCD at an appropriate distance scale. This matching is made possible by defining the perturbative potentials through Fourier transforms with a low-momentum cutoff. The central (spin-independent) potential is compared with potentials derived from an expansion in powers of the inverse quark mass. A well-controlled continuation of the charmonium spin-spin potential from lattice QCD to short distances is performed. The mass splittings of the charmonium singlet and triplet states below the open charm threshold, obtained from the matched spin-spin potential, are in good agreement with the experimental values.

I. INTRODUCTION

Within the framework of potential non-relativistic QCD (pNRQCD) the heavy-quark-antiquark potential is a well-defined quantity, and usually presented as an expansion in powers of the inverse heavy-quark mass [1]. The leading-order static potential (i.e., the potential between infinitely heavy quarks) is accurately known from lattice QCD studies. The potentials at order $1/m$ and $1/m^2$ have been computed in quenched lattice QCD using the Wilson-loop formalism [2–4]. In this approach, a spin-spin potential is found at order $1/m^2$ with a sign such that the mass ordering of hyperfine multiplets is opposite to the ordering observed empirically. An earlier extraction of the spin-spin potential from lattice QCD [5] found a sign in agreement with the empirical ordering.

A different lattice QCD approach to extract the heavy-quark potentials has recently been proposed in Ref. [6]. The spin-spin and central potentials at finite quark mass are obtained from Nambu-Bethe-Salpeter (NBS) amplitudes through an effective Schrödinger equation. A repulsive spin-spin potential which shifts spin triplet states upward and spin singlet states downward is found as required for reproducing the experimental charmonium and bottomonium spectra. Although some model dependence is involved in this approach, the resulting shape of the potential is quite different from a δ -function potential that one commonly obtains from one-gluon exchange with an effective coupling strength α_s treated as an adjustable parameter.

In this Letter we show that one-gluon exchange is, in fact, sufficient to derive a perturbative spin-spin potential, consistent with the recent findings in lattice QCD, if the running of the QCD coupling $\alpha_s(q)$ is properly included. A matching of perturbative and non-perturbative regions of the spin-spin potential is thus possible. The central (spin-independent) charmonium potential, obtained in full lattice QCD from NBS amplitudes, is matched to a corresponding perturbative potential and compared with results obtained previously in the $1/m$ expansion [7]. The perturbative potentials are constructed with a restricted Fourier transformation. This method replaces the frequently used renormalon subtraction

scheme [8]. The S-wave charmonium spectrum is derived in Section III from the combination of the matched central and spin-spin potentials and compared with experimental values. The single free parameter in our approach is an overall additive constant which enters in the extraction of the charm-quark mass.

II. CONSTRUCTION AND COMPARISON OF CHARMONIUM POTENTIALS

The quark-antiquark potential is commonly written in the form

$$V_{q\bar{q}}(r) = V_C(r) + \vec{S}_q \cdot \vec{S}_{\bar{q}} V_S(r) + \dots, \quad (1)$$

with a central potential $V_C(r)$ and a spin-spin potential $V_S(r)$. First, consider the perturbative central (spin-independent) charmonium potential. As in Ref. [7], we define it in r -space via a restricted Fourier transformation with a low-momentum cutoff μ_C :

$$V_C^{\text{pert}}(r, \mu_C) = \int_{q > \mu_C} \frac{d^3 q}{(2\pi)^3} e^{i\vec{q} \cdot \vec{r}} \left[\tilde{V}^{(0)}(q) + \frac{\tilde{V}^{(1)}(q)}{m/2} \right], \quad (2)$$

with $q = |\vec{q}|$. It includes the static potential $\tilde{V}^{(0)}(q)$ at two-loop order in momentum space

$$\tilde{V}^{(0)}(q) = -\frac{16\pi\alpha_s(q)}{3q^2} \left[1 + \frac{\alpha_s(q)}{4\pi} a_1 + \frac{\alpha_s^2(q)}{(4\pi)^2} a_2 \right], \quad (3)$$

and the $1/m$ potential at leading order [9]:

$$\tilde{V}^{(1)}(q) = -\frac{2\pi^2\alpha_s^2(q)}{q}. \quad (4)$$

The coefficients a_1 and a_2 in Eq. (3) are known analytically [10–12] and have the values

$$a_1 = 7, \quad (5)$$

$$a_2 = \frac{695}{6} + 36\pi^2 - \frac{9}{4}\pi^4 + 14\zeta(3), \quad (6)$$

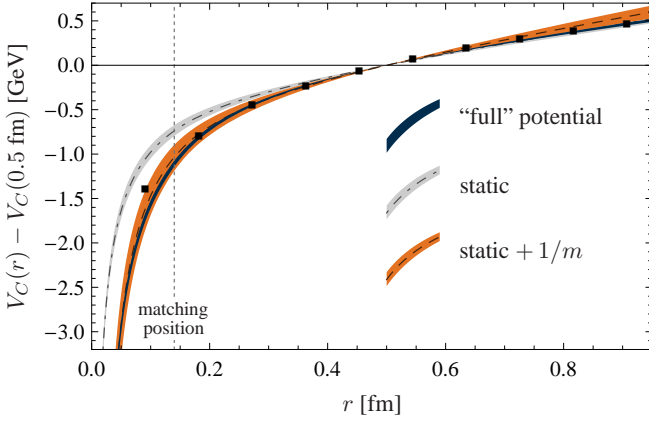


FIG. 1. Charmonium potential from a combination of perturbative QCD and lattice QCD [16] matched at $r_m = 0.14$ fm (solid curve). The dot-dashed line (with error band) shows the static potential from Ref. [7] for comparison, while the dashed line (with error band) shows the static-plus- $1/m$ potential from Ref. [7]. The energy scale is chosen relative to the potential at $r = 0.5$ fm for convenience.

for three light quark flavors. The low-momentum region excluded in Eq. (2) is not accessible in perturbation theory. It is substituted by an additive overall constant to the potential (see [7] for details).

The full four-loop renormalization-group (RG) running [13] with three light flavors is implemented for the strong coupling $\alpha_s(q)$. We use the input value $\alpha_s(1.25 \text{ GeV}) = 0.406 \pm 0.010$, derived from $\alpha_s(m_Z = 91.1876 \text{ GeV}) = 0.1184 \pm 0.0007$ [14], taking into account flavor thresholds [15].

The perturbative potential is matched at a suitable distance r_m to the spin-independent potential calculated in full lattice QCD using NBS amplitudes [16]. This lattice potential includes charm-quark mass effects to all orders and can be parametrized as

$$V_C^{\text{lat}}(r) = -\frac{A}{r} + \sigma r + \text{const}, \quad (7)$$

with $A = 0.813 \pm 0.022$ and $\sqrt{\sigma} = (0.394 \pm 0.007) \text{ GeV}$. Optimal matching is achieved with a low-momentum cutoff $\mu_C = (0.54 \pm 0.02) \text{ GeV}$. In the region around the chosen matching position $r_m = 0.14$ fm, the perturbative potential and the lattice potential are both expected to be reliable. The potential changes only marginally under limited variations of the matching point.

In Fig. 1 we compare this matched central potential (solid curve) with the potential obtained in the Wilson-loop approach using a $1/m$ expansion. One observes that the “full” potential differs significantly from the static potential constructed in Ref. [7] (dot-dashed line with error band), but it is consistent within errors when the $1/m$ potential from Ref. [7] is added to the static potential (dashed line with error band). The charm-quark mass m relevant for the $1/m$ potential has been varied in Fig. 1 in the range $(1.5 \pm 0.2) \text{ GeV}$.

Let us now focus on the spin-spin potential. Tensor and spin-orbit terms are not discussed in this Letter. These have so far not been studied in the new lattice QCD approach employing the NBS amplitudes. The authors of Ref. [16] fit the spin-spin potential from full lattice QCD with three different functional forms. We use the exponential form

$$V_S^{\text{lat}}(r) = \alpha e^{-\beta r}, \quad (8)$$

with $\alpha = (0.825 \pm 0.019) \text{ GeV}$ and $\beta = (1.982 \pm 0.024) \text{ GeV}$, since it provides the best fit to the lattice data.

In the following we construct a perturbative spin-spin potential that can be used to continue the lattice potential to short distances. Recall first the well-known (schematic) spin-spin potential derived from one-gluon exchange assuming a constant coupling α_s :

$$V_S(r) = \frac{32\pi}{9m_q^2} \alpha_s \delta^3(\vec{r}), \quad (9)$$

with the quark/antiquark mass m_q . This δ -function term is in agreement with the leading-order spin-spin potential obtained in pNRQCD [1].

In analogy to the case of the spin-independent potential, it is possible to include the RG running of $\alpha_s(q)$ in the construction of the spin-spin potential. We define the perturbative part of $V_S(r)$ as:

$$V_S^{\text{pert}}(r, \mu_S) = \frac{32\pi}{9m^2} \int \frac{d^3q}{(2\pi)^3} e^{i\vec{q}\cdot\vec{r}} \alpha_s(q), \quad (10)$$

with a low-momentum cutoff μ_S . For $q > \mu_S$ the perturbative RG evolution of $\alpha_s(q)$ is supposed to be reliable. The non-perturbative infrared behavior of the quark and gluon couplings prohibits a controlled low-momentum extension for $q < \mu_S$. It is nevertheless useful to examine such an extension for $r \ll 1/\mu_S$ in the form

$$V_S^{\text{ir}} = \frac{32\pi}{9m^2} \bar{\alpha}_s \int \frac{d^3q}{(2\pi)^3} e^{i\vec{q}\cdot\vec{r}} \simeq \frac{16 \bar{\alpha}_s}{27\pi m^2} \mu_S^3, \quad (11)$$

with a parameter $\bar{\alpha}_s$ reflecting the average interaction strength in the infrared region. Note that Eq. (11) gives a positive constant proportional to μ_S^3 to be added as a correction to $V_S^{\text{pert}}(r, \mu_S)$, with $\bar{\alpha}_s$ not known, but expected to be of $\mathcal{O}(1)$.

In order to facilitate the numerical evaluation of the Fourier integral for the perturbative part, it is useful to rewrite $V_S^{\text{pert}}(r, \mu_S)$ in the form

$$V_S^{\text{pert}}(r, \mu_S) = -\frac{16}{9m^2 \pi r} \frac{\partial}{\partial r} \int_{\mu_S}^{\infty} dq \cos(qr) \alpha_s(q). \quad (12)$$

To be consistent with the lattice QCD analysis, the charm-quark mass m in the denominator of Eq. (12) is

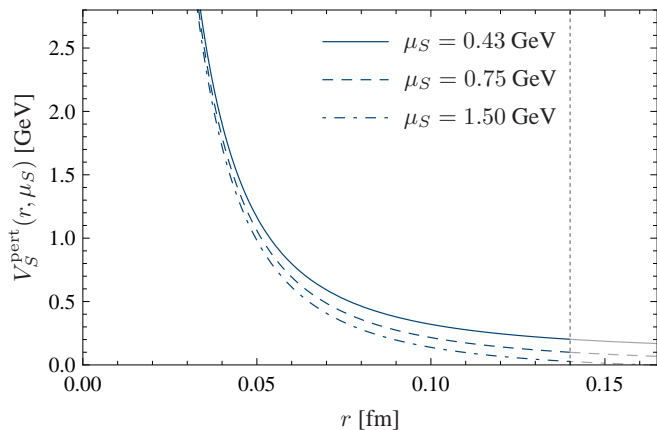


FIG. 2. Spin-spin potential in r -space derived from one-gluon exchange as defined in Eq. (12). The potential is shown for different values of the low-momentum cutoff μ_S .

identified with (1.74 ± 0.03) GeV, the kinetic quark mass that has been determined in Ref. [16]. Discarding the additive constant V_S^{ir} in the first step, the resulting short distance potential and its dependence on the cutoff scale μ_S is shown in Fig. 2. The shape is evidently very different from a Gaussian or a δ -function. Such forms are frequently used for the spin-spin potential in phenomenological models.

The two components of the spin-spin potential, arising from perturbative QCD for $r \leq r_m$ and from lattice QCD for $r \geq r_m$, can be matched at $r_m = 0.14$ fm. When ignoring the additive constant V_S^{ir} this matching is achieved for $\mu_S = (0.43 \pm 0.02)$ GeV. With inclusion of the (variable) additive constant V_S^{ir} the infrared cutoff μ_S can be varied over a wide range almost without any effect on the spin-spin potential. Figure 3 shows the matched potential with an infrared cutoff of $\mu_S = (0.75 \pm 0.25)$ GeV.

III. SPECTROSCOPY AND CHARM-QUARK MASS

Here, we discuss the charmonium spectrum below the $D\bar{D}$ threshold as derived from the matched potentials constructed in the previous section. We focus on the 1S and 2S states which are not influenced by the tensor and spin-orbit interactions. The Schrödinger equation for these states,

$$\left[-\frac{\vec{\nabla}^2}{m} + 2m_{\text{PS}}(\mu_C) + V_C(r) + \vec{S}_q \cdot \vec{S}_{\bar{q}} V_S(r) - E \right] \psi(\vec{r}) = 0, \quad (13)$$

involves a single free parameter $m_{\text{PS}}(\mu_C)$, the (μ_C -dependent) charm-quark mass in the potential subtracted (PS) scheme [17]. In order to make the PS scheme applicable for our purposes, we extend it by including the

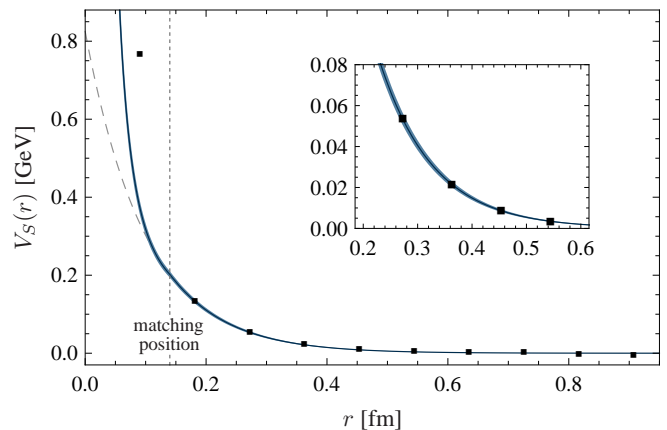


FIG. 3. Charmonium spin-spin potential (with error band) from a combination of perturbative QCD (see Eq. (12)) and lattice QCD [16], matched at $r_m = 0.14$ fm. Dashed line: continuation of the exponential lattice fit (8) to short distances.

$1/m$ -correction term:

$$m_{\text{PS}}(\mu_C) = m_{\text{pole}} + \frac{1}{2} \int \frac{d^3q}{(2\pi)^3} \left[\tilde{V}^{(0)}(q) + \frac{\tilde{V}^{(1)}(q)}{m/2} \right]. \quad (14)$$

Replacing the operator $\vec{S}_q \cdot \vec{S}_{\bar{q}}$ by its eigenvalues, $-3/4$ for the spin singlet and $1/4$ for the spin triplet, the Schrödinger equation (13) is solved numerically. The spin-spin potential $V_S(r)$ can be included in two different ways. In the first case it is treated in first-order perturbation theory, in the second case it is fully included in the Schrödinger equation. Due to the singular behavior of $V_S(r) \sim r^{-2.8}$ for $r \rightarrow 0$ (according to our construction) the wave functions diverge (mildly) in the latter case for very small values of r . In this case we solve the radial Schrödinger equation numerically for $r > 0.003$ fm and convince ourselves that the physical results are not affected by contributions coming from shorter distances. The results of the two alternative treatments of the spin-spin potential agree within 12 MeV (see Table I). The calculated mass splittings between singlet and triplet states are in good agreement with experimental results for both 1S and 2S charmonia.

The single free parameter $m_{\text{PS}}(\mu_C)$ is chosen such that the spin-weighted average of the 1S states agrees with its

	Case 1	Case 2	Experiment [18]
1S mass splitting [MeV]	117 ± 6	105 ± 6	116.6 ± 1.2
2S mass splitting [MeV]	56 ± 3	46 ± 3	49 ± 4

TABLE I. Predicted mass splittings of charmonium 1S and 2S multiplets in comparison with experimental data. Case 1: spin-spin potential treated in first-order perturbation theory. Case 2: spin-spin potential fully included in the Schrödinger equation.

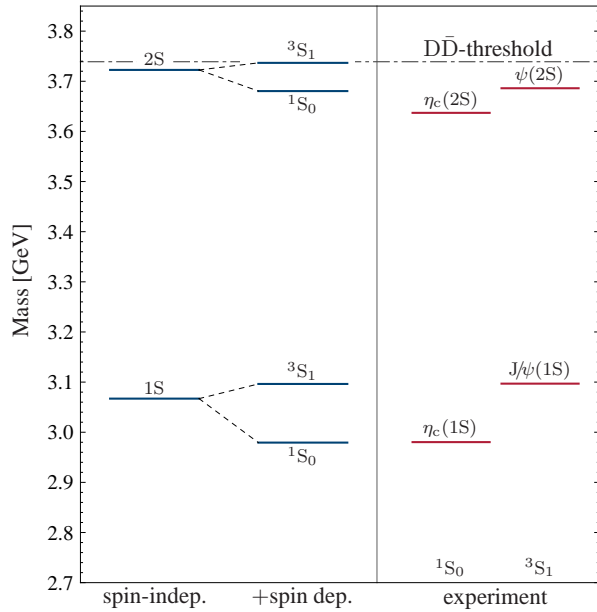


FIG. 4. Predicted masses of charmonium 1S and 2S states in comparison with experimental data [18]. The results in the first column are based on the spin-independent potential only. The effects of the spin-spin potential, treated in first-order perturbation theory, are added in the second column.

experimental value [18]. For the excited 2S states our approach predicts masses for $\eta_c(2S)$ and $\psi(2S)$ that are slightly too large (see Fig. 4). However, these states are close to the $D\bar{D}$ threshold. Going beyond this threshold requires a complex (energy-dependent) $c\bar{c}$ potential or an explicit treatment of coupled channels. While the imaginary part starts at the opening of the $D\bar{D}$ channel, the corresponding dispersive real part induces an attractive shift of the 2S states. In second-order perturbation theory this shift is proportional to the squared $c\bar{c} \rightarrow D\bar{D}$ transition matrix element.

The predicted size of the hyperfine splittings is quite sensitive to the value of the mass m in the denominator of Eq. (12). For example, choosing $m = 1.5$ GeV instead of the kinetic quark mass (1.74 ± 0.03) GeV [16] would give rise to a 1S mass splitting that is about 20% too large. This is in contrast to variations of the matching position r_m and the infrared cutoff μ_S , which affect the hyperfine splittings only marginally.

The spin-spin potential, as constructed in the previous section, produces a non-vanishing but small splitting between the 1P singlet and triplet states, namely $h_c(1P)$ and $\chi_{c1}(1P)$, unlike the δ -function spin-spin potential. In first-order perturbation theory the effect amounts to a mass difference of (8.2 ± 0.5) MeV. The full inclusion of the spin-spin potential $V_S(r)$ in the Schrödinger equation gives rise to a slightly larger mass splitting of (8.3 ± 0.5) MeV.

The value of the mass parameter $m_{PS}(\mu_C)$, determined in our approach by fitting to empirical charmonium spectra, can be translated into alternative schemes for quark masses. The PS mass $m_{PS}(\mu_C)$ is first converted to the

pole mass and in a second step mapped onto the \overline{MS} mass $\overline{m}_c \equiv m_{\overline{MS}}(m_{\overline{MS}})$. This procedure is described in detail in Ref. [7]. Applying the same method here, we find for the charm-quark mass in the \overline{MS} scheme

$$\overline{m}_c = (1.21 \pm 0.04) \text{ GeV}, \quad (15)$$

in good agreement with other determinations [7, 18]. The error reflects combined uncertainties in the lattice potentials, in the input value of the strong coupling $\alpha_s(q)$, and from the matching to the empirical states.

We close with a few remarks concerning bottomonium: until now, the bottomonium spin-spin potential has not been studied within the new lattice QCD approach based on NBS amplitudes. An extrapolation of the spin-spin potential from charmonium to bottomonium can be done by simply assuming a $1/m^2$ dependence of the lattice potential and allowing for variations of the mass parameter m . In the perturbative part of the potential we account furthermore for a modified running of $\alpha_s(q)$ due to four massless flavors and use $\alpha_s(4.2 \text{ GeV}) = 0.226 \pm 0.003$ as an input. The empirical mass splitting of (69 ± 3) MeV [18] between $\eta_b(1S)$ and $\Upsilon(1S)$ can be reproduced either for a kinetic bottom-quark mass $m = 4.7$ GeV (with the spin-spin potential treated in first-order perturbation theory), or with $m = 4.3$ GeV (if the spin-spin potential is fully included in the Schrödinger equation). It will be interesting to have available the corresponding lattice QCD results for bottomonium.

IV. SUMMARY

Central and spin-spin potentials for charmonium have been derived by combining perturbative QCD at small distances ($r < 0.14$ fm) with results from lattice QCD for larger distances up to $r \simeq 1$ fm. By defining the perturbative potentials via a restricted Fourier transformation this matching has been made possible. We have found that the central quark-antiquark potential, constructed from NBS amplitudes in full QCD lattice simulations [6, 16], agrees within errors with the static-plus- $1/m$ potential derived in the Wilson-loop formalism [2–4]. The matched spin-spin potential produces hyperfine splittings for the S-wave charmonium states that are in good agreement with experiment. The \overline{MS} mass of the charm quark also agrees well with other determinations of this QCD parameter.

ACKNOWLEDGMENTS

This work was supported in part by BMBF, GSI and the DFG Excellence Cluster “Origin and Structure of the Universe”. We thank Antonio Vairo for useful discussions. One of the authors (A.L.) acknowledges partial support by the TUM Graduate School.

-
- [1] N. Brambilla, A. Pineda, J. Soto, and A. Vairo, Rev. Mod. Phys. **77**, 1423 (2005).
 - [2] Y. Koma, M. Koma, and H. Wittig, Phys. Rev. Lett. **97**, 122003 (2006).
 - [3] Y. Koma and M. Koma, Nucl. Phys. **B769**, 79 (2007).
 - [4] Y. Koma, M. Koma, and H. Wittig, PoS **LAT2007**, 111 (2007).
 - [5] G. S. Bali, K. Schilling, and A. Wachter, Phys. Rev. **D56**, 2566 (1997).
 - [6] T. Kawanai and S. Sasaki, Phys. Rev. Lett. **107**, 091601 (2011).
 - [7] A. Laschka, N. Kaiser, and W. Weise, Phys. Rev. **D83**, 094002 (2011).
 - [8] A. Pineda, JHEP **0106**, 022 (2001).
 - [9] N. Brambilla, A. Pineda, J. Soto, and A. Vairo, Phys. Rev. **D63**, 014023 (2000).
 - [10] M. Peter, Phys. Rev. Lett. **78**, 602 (1997).
 - [11] M. Peter, Nucl. Phys. **B501**, 471 (1997).
 - [12] Y. Schröder, Phys. Lett. **B447**, 321 (1999).
 - [13] T. van Ritbergen, J. A. M. Vermaseren, and S. A. Larin, Phys. Lett. **B400**, 379 (1997).
 - [14] S. Bethke, Eur. Phys. J. **C64**, 689 (2009).
 - [15] K. G. Chetyrkin, B. A. Kniehl, and M. Steinhauser, Phys. Rev. Lett. **79**, 2184 (1997).
 - [16] T. Kawanai and S. Sasaki, Phys. Rev. **D85**, 091503(R) (2012).
 - [17] M. Beneke, Phys. Lett. **B434**, 115 (1998).
 - [18] Particle Data Group, K. Nakamura *et al.*, J. Phys. **G37**, 075021 (2010).